Indian Journal of Science and Technology, Vol 10(5), DOI: 10.17485/ijst/2017/v10i5/111139, February 2017
ISSN (Print) : 0974-6846
ISSN (Online) : 0974-5645

Modelling and Simulation of Photovoltaic System Fed Two Input Two Output DC-DC Boost Converter Interfaced with Asymmetric Cascaded H-Bridge Multilevel Inverter

S. Augusti Lindiya[1]*, S. Palani[2], K. Vijayarekha[1]

[1]Department of Electrical and Electronics Engineering, SASTRA University, Tirumalaisamudram, Thanjavur - 613 401, Tamilnadu, India; lindiya@eee.sastra.edu, vijayarekha@ee.sastra.edu
[2]Department of Electrical and Electronics Engineering, Sudharsan College of Engineering, Sathiyamangalam - 622501, Tamil Nadu, India; Keeranur_palani@yahoo.com

Abstract

Objectives: Multiple Input Multiple Output dc-dc boost converters is used to interface diversified renewable energy sources to Asymmetric Cascaded H-Bridge Multilevel Inverter whose output voltages can be connected to the grid system. The compensators and/or controllers are required to provide the constant output voltages of the boost converter against disturbances along with desired time domain specifications. In this paper, two input two output dc-dc boost converter is developed to interface with seven level multilevel inverter. **Methods/Statistical Analysis:** One of the input sources is replaced by Photovoltaic panel and Incremental Conductance based Maximum Power Point Tracking Algorithm is developed to improve the efficiency of the system. Compensators are designed to maintain the constant output voltages of the converter against disturbances using transfer function model obtained from developed small signal model of the converter. The developed system is simulated using MATLAB /Simulink and the total harmonic distortion in the output voltage of the inverter is observed .The simulated closed loop output voltages of the dc-dc converter are validated by developing prototype model of the converter using AT 89C51 microcontroller. **Findings:** It is found that the two input two output dc-dc converter provides constant dc voltages to the asymmetric multilevel inverter from the diversified energy sources with improved time domain specifications using compensators. **Application/Improvements:** The designed system is having the applications in renewable power system, aerospace power systems and hybrid energy vehicle.

Keywords: Compensators, MPPT Algorithm, Multilevel Inverter, Photovoltaic Panel, Small Signal Modeling, THD

1. Introduction

The conventional energy sources are rapidly depleting. Moreover the cost of energy is rising and therefore renewable energy sources is a promising alternative. They are sustainable, needless maintenance and have low environmental impacts. The PV array converts the sunlight into electricity. PV array is a combination of series and parallel PV cells[1]. Depending upon the atmospheric conditions such as solar irradiation and temperature, electrical power is generated. Due to the changes in atmospheric condition, extracting maximum power from the PV panel is necessary so MPPT algorithm with the help of mathematical model[2] is applied to the PV panel in order to improve the efficiency of the system[3,4]. Also, due to the intermittent nature of renewable energy sources, a MIMO system is considered such that maximum utilization of energy sources is possible. A Boost MIMO converter is

*Author for correspondence

one of the most efficient techniques considered to step up the low input voltage to a higher needed DC output voltage[5]. Renewable sources can be connected to the power grid only through inverters[6]. The main aim of the industries is to have less production cost with high efficiency. There are many types of inverters, among them multilevel inverters are mostly required for industries because of its medium and high power operations with reduced harmonic distortion[7]. By increasing the number of levels, the output waveforms produced by the inverter will have more steps which are closer to sine waveform. Among the various multilevel inverter types, CHB-MLI is the most widely used multilevel inverter. Since the output voltage from the converter is obtained in the form of E and 2E asymmetric CHB-MLI is used. Asymmetric CHB-MLI has many advantages compared with symmetric CHB-MLI such as for same number of input dc sources, the output voltage levels are increased with reduced number of switches[8]. Therefore the asymmetric topologies allow generating more voltage levels with less semiconductor switches and also its efficiency and reliability is improved. The overall block diagram for asymmetric CHB-MLI fed from MIMO DC-DC boost converter is represented in Figure1.

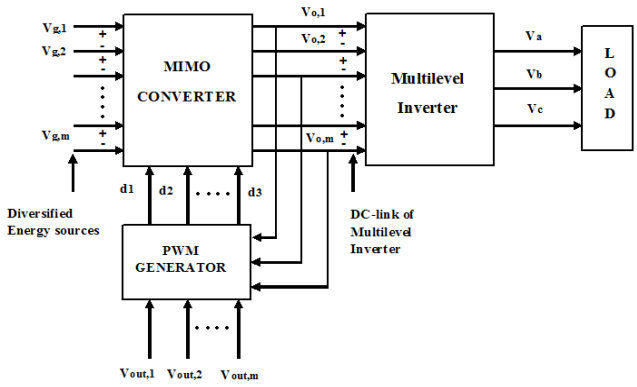

Figure 1. Block diagram of proposed system.

2. PV Modeling

$$I = I_{pv} - I_0\left[exp\left(\frac{V + R_s I}{V_t a}\right) - 1\right] - \frac{V + R_s I}{R_p} \quad (1)$$

$$I_{pv} = \frac{(I_{pv,n} + K_I \Delta_T)V}{G_n} \quad (2)$$

Equivalent circuit for PV cell is represented in Figure 2.The *I-V* characteristics of PV cell can be mathematically described as,

$$I_0 = \frac{I_{sc,n} + K_I \Delta_T}{exp\left(\frac{V_{oc,n} + K_V \Delta_T}{aV_t}\right) - 1} \quad (3)$$

$$V_t = \left(\frac{N_s KT}{q}\right) \quad (4)$$

$$\Delta_T = T - T_n \quad (5)$$

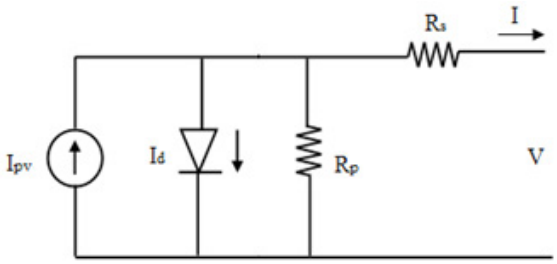

Figure 2. Equivalent circuit for PV cell.

Table1 shows the Electrical characteristics data of Kyocera®KC85T PV module[9]. I-V characteristics of the PV array is non-linear and the open circuit voltage V_{oc} and short circuit current I_{sc} are shown in Figure 3 in which both points have power generation as zero but there is a point in which PV cell generates the maximum power. Due to the change in atmospheric condition, extracting maximum power from the PV panel is necessary which can be done by applying MPPT algorithm to the PV panel in order to improve the efficiency of the system. Among the various MPPT techniques, incremental conductance is the most widely used method because of its low complexity and also it can track the fast changing atmospheric condition more accurately

Table 1. Electrical Characteristics data of KC85TPV Module

Label	Description
Maximum Voltage (V_{mp})	17.4 V
Maximum Current (I_{mp})	5.02 A
Series Resistance (R_s)	0.221 Ω
Parallel Resistance (R_p)	415.405 Ω
Nominal Temperature (T_n)	25^0 C
Nominal Irradiation (G_n)	1000W/m^2
Bandgap Energy (E_g)	1.12 ev
Short Circuit Current (I_{sc})	5.34 A
Open Circuit Voltage (V_{oc})	21.7 V
Diode ideality constant (a)	1.3

Electron charge (Q)	1.60217646 x 10^{-19} C
Boltzmann constant (K)	1.3806503 x 10^{-23} J/K

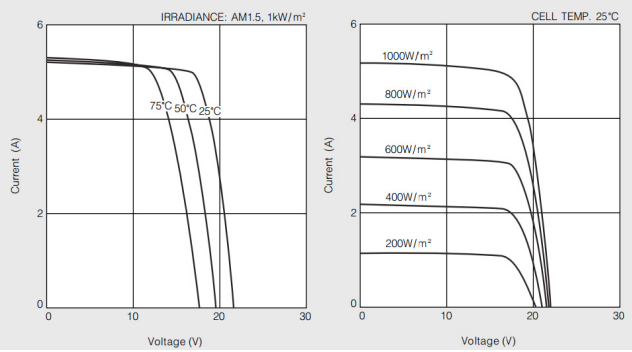

Figure 3. I-V and P-V characteristics of PV array.

When compared to other algorithm. The derivative of the output power with respect to the PV voltage and current is calculated in this method. At MPP the slope of PV curve is zero. Figure 4 shows the flow chart for incremental conductance method.

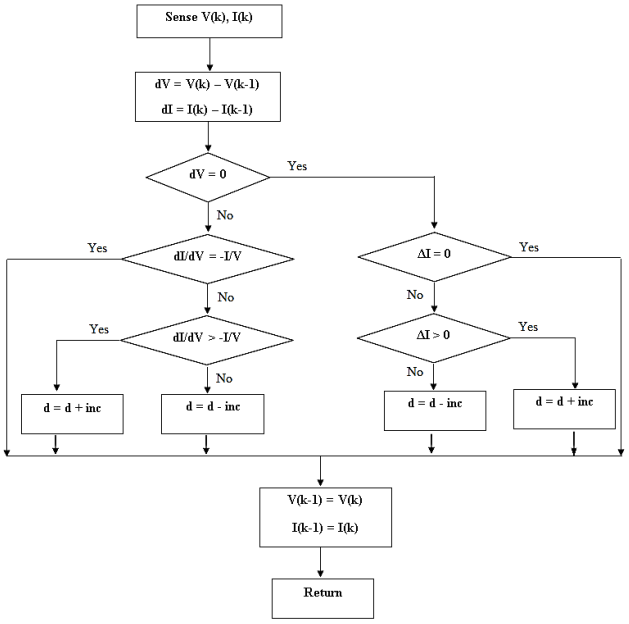

Figure 4. Flow chart for incremental conductance algorithm.

$$\left(\frac{dP}{dV}\right)_{mpp} = \left(\frac{d(VI)}{dV}\right) \tag{6}$$

$$0 = I + \frac{V.dI}{dV_{mpp}} \tag{7}$$

$$\frac{dI}{dV_{mpp}} = \frac{-I}{V} \tag{8}$$

3. Converter Modeling

Circuit diagram for two input two outputs DC-DC boost converter is shown in Figure 5. It consists of two input sources V_{in1} and V_{in2} with the condition $V_{in1}<V_{in2}$ such that the operation can be simplified. It has three switches (S_1, $S2and$ S_3), three diodes (D_0, $D_1$and D_2) and two capacitors ($C_1$and C_2). Pulses for the switches and voltage and current waveforms of the inductor are shown in Figure 6. According to the switching pattern there are four different modes of operation which are explained in Table 2. Mathematical model of the converter is required to design controller such that the output voltages are maintained constant against load disturbances[10,11]. According to the small signal modeling method the input voltages, duty ratios and the state variables have its DC values and perturbations[12]. Thus, based on state space averaging method applied to the equations obtained from four different modes of operation, equation (9) is obtained.

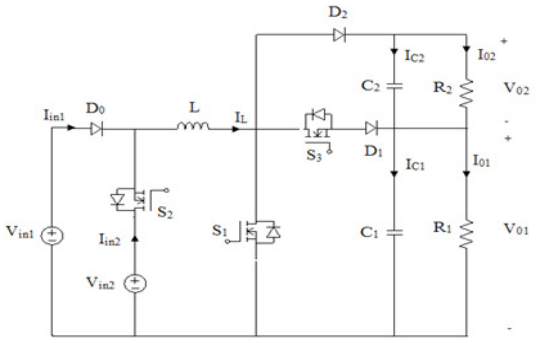

Figure 5. Two input two output DC-DC boost converter.

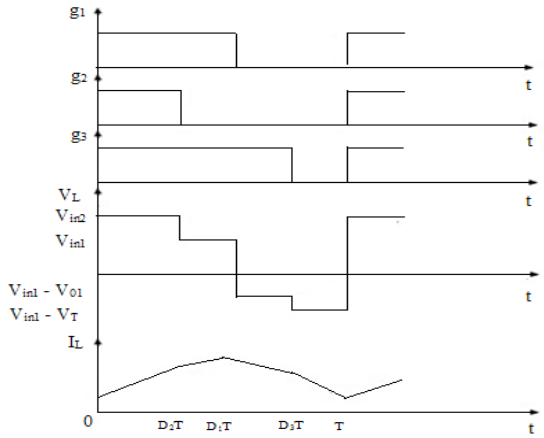

Figure 6. Steady state waveforms of the proposed converter.

Table 2. Switching States of Dual Input Dual Output dc-dc Boost Converter

Switching state	Interval	S_1	S_2	S_3
1	$0 < t < D_2T$	ON	ON	OFF
2	$D_2T < t < D_1T$	ON	OFF	OFF
3	$D_1T < t < D_3T$	OFF	OFF	ON
4	$D_3T < t < T$	OFF	OFF	OFF

$$(1 - D_1)\hat{V}_{o1}(t) + (D_3 - 1)\hat{V}_{o2} + V_{01}\hat{d}_1(t) + V \quad (9)$$

$$C_1\frac{d\hat{V}_{o1}(t)}{dt} = -I_L\hat{d}_1(t) + (1 - D_1)\hat{\imath}_L(t) - \frac{\hat{V}_{o1}(t)}{R_1} \quad (10)$$

$$C_2\frac{d\hat{V}_{o2}(t)}{dt} = -I_L\hat{d}_3(t) + (1 - D_3)\hat{\imath}_L(t) - \frac{\hat{V}_{o2}(t)}{R_2} \quad (11)$$

Switching period for S_1, S_2 and S_3 are found from equation (10) which is the steady state equation.

$$\begin{bmatrix} V_{01} & V_{in2} - V_{in1} & V_{02} \\ R_1I_b & V_{01} & 0 \\ 0 & V_{01} & R_2I_b \end{bmatrix}\begin{bmatrix} D_1 \\ D_2 \\ D_3 \end{bmatrix} = \begin{bmatrix} V_{02} + V_{01} - V_{in} \\ R_1I_b \\ R_2I_b \end{bmatrix} \quad (12)$$

The state space model of the proposed converter is given in the equation (11) and (12).

(13)

$$\begin{bmatrix} \hat{\imath}_L \\ \hat{V}_{01} \\ \hat{V}_{02} \end{bmatrix} = \begin{bmatrix} 0 & 1 & 0 \\ 0 & 1 & 0 \\ D_3 & 0 & 1 \end{bmatrix}\begin{bmatrix} \hat{\imath}_L \\ \hat{V}_{01} \\ \hat{V}_{02} \end{bmatrix} + \begin{bmatrix} 0 & 0 & 0 \\ 0 & 0 & 0 \\ 0 & I_L & 0 \end{bmatrix}\begin{bmatrix} \hat{d}_3 \\ \hat{d}_1 \\ \hat{d}_2 \end{bmatrix} \quad (14)$$

The transfer functions are obtained as,

$$g_{11} = \frac{\hat{V}_{01}(s)}{d_3(s)}$$

(15)

$$g_{22} = \frac{\hat{V}_T(s)}{d_2(s)}$$

$$L + (1 - D_1)^2R_1R_2C_1 + (D_3 - 1)^{\square}\tau \quad (16)$$

$$g_{33} = \frac{\hat{I}_{in2}(s)}{d_1(s)}$$

$$R_1C_1R_2C_{\square 1} \quad (17)$$

Thus from the transfer functions (15), (16) and (17) it is obviously seen that the output voltages V_{01} and V_T are controlled by controlling the duty cycles d_3 and d_2 respectively. The specifications which are designed and used in the model are given in Table 3.The values specified in Table4 are substituted in the transfer functions g_{11}, g_{12} and is obtained as,

$$g_{11} = \frac{\hat{V}_{01}(S)}{d_3(s)} = \frac{396428.57S + 10262059.37}{s^3 + 41.558s^2 + 3950.60s + 52179.96} \quad (19)$$

$$g_{22} = \frac{\hat{V}_T(s)}{d_2(s)} = \frac{157791.68S + 250463}{s^3 + 41.558s^2 + 3950.60s +} \quad (20)$$

Table 4. Specifications of Two Input Two Output dc-dc Boost Converter

Parameters	Values
Input Voltage 1 (V_{in1})	24V
Input Voltage 2 (V_{in2})	36V
Inductor (L)	28mH
Capacitor (C_1 and C_2)	1000μF and 2200μF
Resistor (R_1 and R_2)	35Ω and 35Ω
Switching Frequency (F_{sw})	10kHZ
Output Voltage (V_{01})	80V
Output Voltage (V_{02})	40V

This converter is interfaced with asymmetric CHB-MLI. Seven level asymmetric CHB-MLI is represented in Figure 7. Asymmetric CHB-MLI has many advantages compared with symmetric CHB-MLI such as for same number of input dc sources, the number of switches used is reduced and the output voltage levels are increased. For example to generate a 7 level output voltage an asymmetric inverter requires only two cells whereas symmetric inverter requires four cells. Therefore the asymmetric topologies allow generating more voltage levels with less semiconductor switches and also efficiency and reliability is improved[13,14]. The new Pulse Width Modulation tech-

Table 3. Charging-discharging and inductor current for various switching states

Switching state	Interval	C_1	C_2	I_L
1	$0 < t < D_2T$	Discharges	Discharges	Increases
2	$D_2T<t<D_1T$	Discharges	Discharges	Increases
3	$D_1T <t<D_3T$	Charges	Discharges	Decreases
4	$D_3T<t<T$	Charges	Discharges	Decreases

niques are developed for grid connected photovoltaic inverter[15,16]. Table 5 shows the switching state of two cell seven level CHB-MLI.

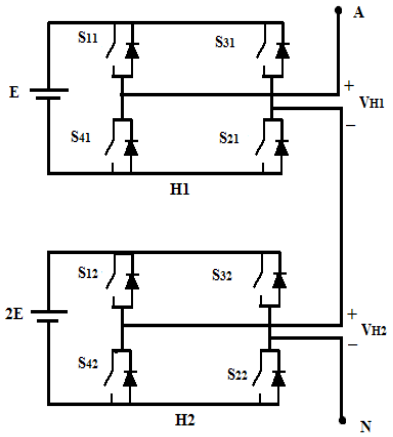

Figure 7. Seven level asymmetric CHB-MLI.

Table 5. Switching State of Two Cell Seven Level CHB- MLI

Output voltage V_{AN}	Switching State					
	S_{11}	S_{31}	S_{12}	S_{32}	V_{H1}	V_{H2}
3E	1	0	1	0	E	2E
2E	1	1	1	0	0	2E
	0	0	1	0	0	2E
E	1	0	1	1	E	0
	1	0	0	0	E	0
	0	1	1	0	-E	2E
0	0	0	0	0	0	0
	0	0	1	1	0	0
	1	1	0	0	0	0
	1	1	1	1	0	0
-E	1	0	0	1	E	-2E
	0	1	1	1	-E	0
	0	1	0	0	-E	0
-2E	1	1	0	1	0	-2E
	0	0	0	1	0	-2E
-3E	0	1	0	1	-E	-2E

4. Control Strategy

The need for control system design of MIMO DC-DC boost converter system is to maintain the constant output voltage. Using compensators stability of the system can be increased and the steady state error can be eliminated. Lead, Lag, Lead/Lag are the types of compensators[17]. These are designed in the form of transfer functions using SISO® tool in MATLAB/Simulink®[18]. Using the transfer functionsg_{11} and g_{12}obtained from small signal modeling method, compensators are designed for switches $S_2$and S_3. Bode plot obtained before applying compensator for$g_{11}$is shown in Figure 8(a). The phase margin of the system obtained is 1.12 deg. which is very low so to increase the phase margin a lead compensator is designed using frequency response and is given in equation (21).

$$G_{11}(S) = 1000\frac{(S+1)}{(S+21200)} \quad (21)$$

Bode plot obtained after applying compensator for $g_1$is shown in Figure 8(b). Thus the phase margin of the system is improved to 54.4 degree.

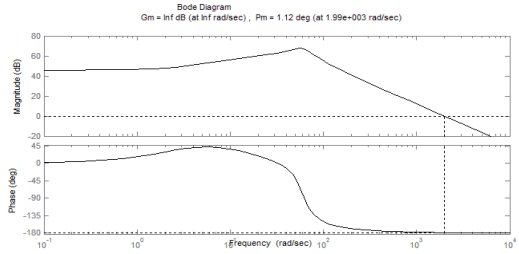

(a)

Figure 8. Bode plot of g_{11} obtained (a) before applying compensator.

Bode plot obtained for g_{22} before applying compensator is shown in Figure 9(a). It shows that the phase margin of the system obtained 3.75 deg which is very low so to increase the phase margin a lead compensator is designed using frequency response and is given in equation (22).

$$G_{22}(s) = 9\frac{(S+15)}{(S+1000)} \quad (22)$$

Bode plot obtained after applying compensator for $g_{22}$is shown in Figure 9(b). Thus the phase margin of the system and system stability is improved to 45.5 degrees.

5. Simulation Results

The performance of the proposed converter has been done by using MATLAB/Simulink® software. The various analytical equations governing the PV cell are modelled and simulated (Figure 10). The obtained *I* -*V* and *P* - *I* characteristics nonlinear curves are shown in Figure

11. MPPT algorithm based on incremental conductance method is developed and applied for PV model to improve the efficiency of the system. The output voltage obtained from PV panel after applying MPPT is shown in Figure 12. This serves as one of the input for two input two outputs DC-DC boost converter. The converter system produces regulated output voltages and is fed to the inverter. Simulation results across the inductor of the converter is measured and obtained as shown in Figure 13. The output voltages measured across the converter is shown in Figure 14. Since it is boost converter the total output voltage required to obtain is 120V that is 80V and 40V across the loads $R_1$and R_2 respectively but only 76V and 34V is obtained. So to produce a regulated output voltage compensators are used. The simulation results of closed loop control for two input two output DC-DC boost converter is shown in Figure 15. In order to verify the performance of controller, disturbances are given to load current. Figure 16 shows that under closed loop condition even though disturbances are given, the output voltage is maintained constant, but it takes 0.1 Sec to settle. Asymmetric CHB-MLI is designed and interfaced with two inputs two outputs DC-DC boost converter. Phase voltage of seven level cascaded multilevel inverter is shown in Figure 17. FFT analysis done for the output voltage of proposed system and is shown in Figure 18. This shows that the harmonic distortion obtained is less.

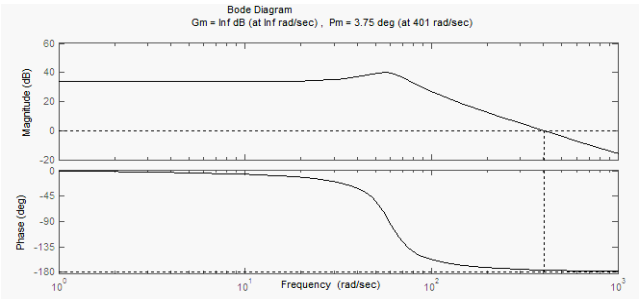

(a)

Figure 9. Bode plot of g_{22} obtained (a) before applying compensator.

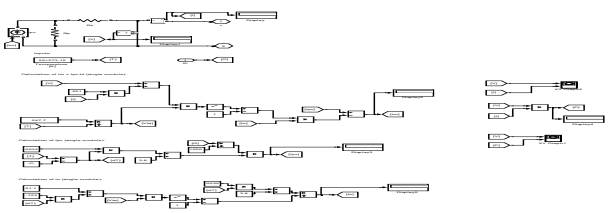

(a)

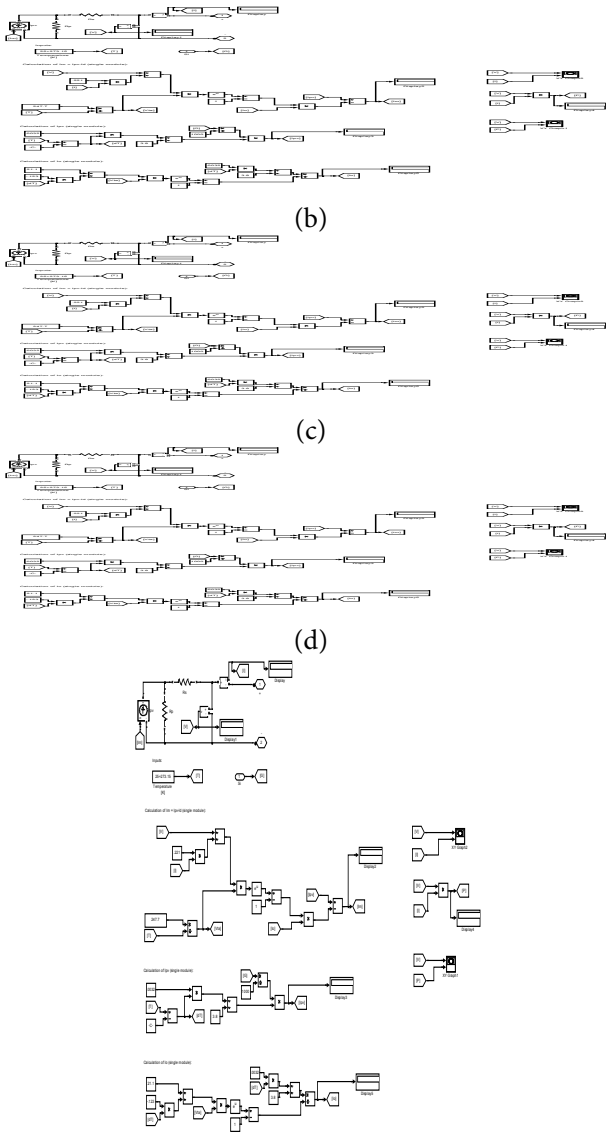

(b)

(c)

(d)

(e)

Figure 10. Modelling of PV cell.

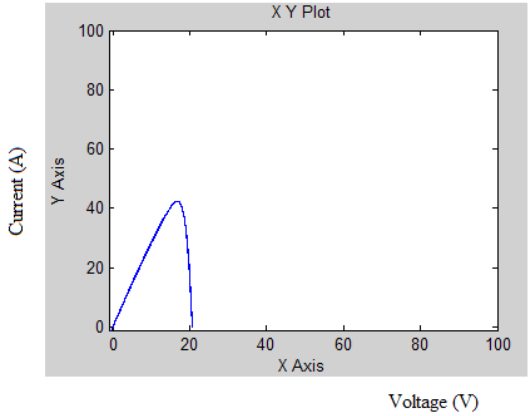

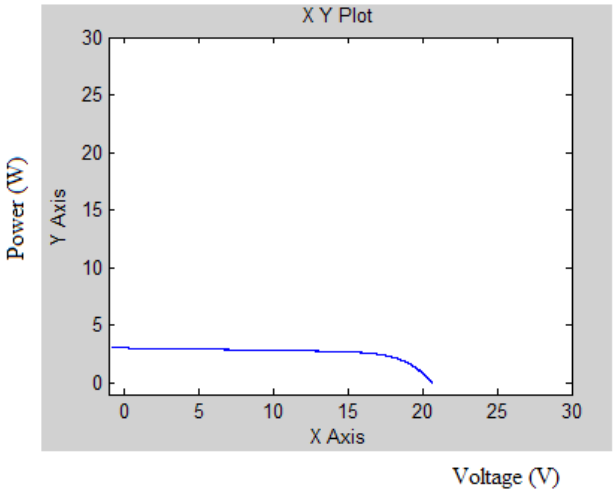

Figure 11. I-V and P-I characteristics of PV cell.

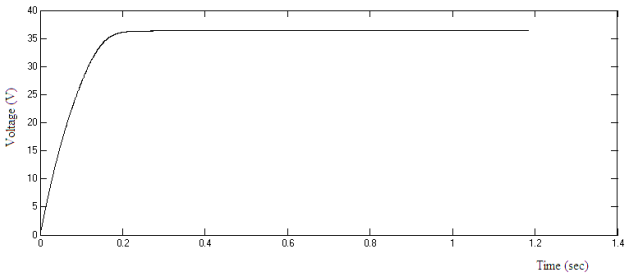

Figure 12. Output voltage obtained from PV panel.

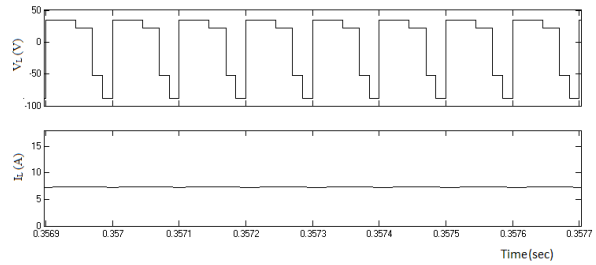

Figure 13. Simulation results across the inductor of the converter.

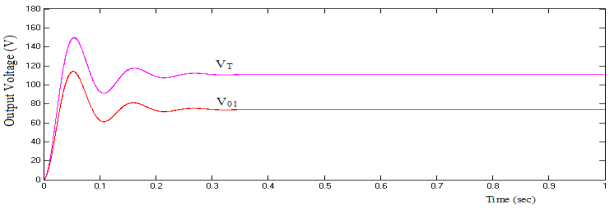

Figure 14. Output voltage waveform of the converter under open loop condition.

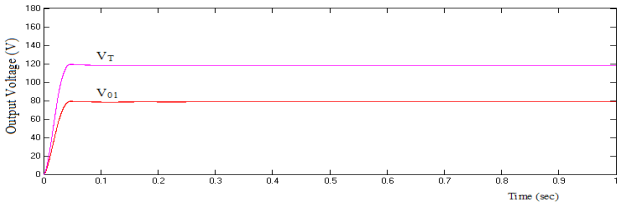

Figure 15. Output voltage waveforms of the converter under closed loop condition.

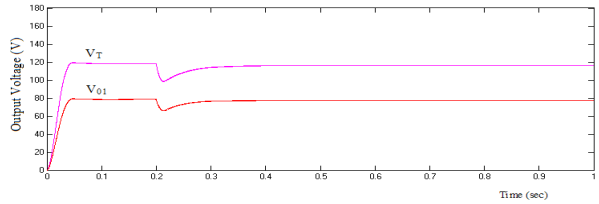

Figure 16. Output voltage waveforms of the converter under disturbances.

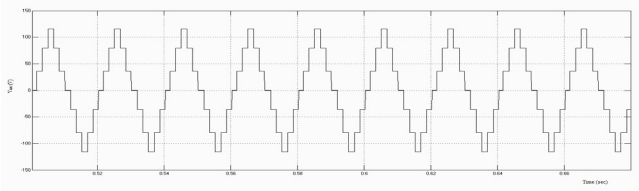

Figure 17. Phase voltage of seven level cascaded multilevel inverter converter system.

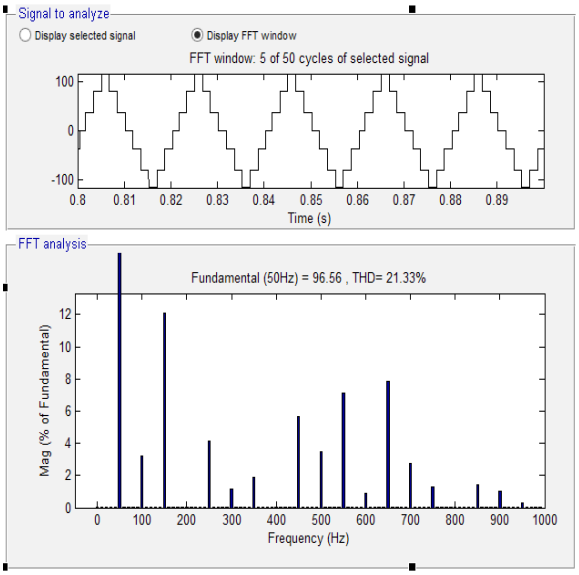

Figure 18. FFT analysis for the output voltage of proposed system.

6. Hardware Implementation

This section describes the hardware implementation of closed loop two input two output DC-DC boost converter. Figure 19 represents the hardware block diagram for closed loop system. The components shown in Table 6 are used to develop the hardware circuit. The power circuit of the converter system requires the driver circuit to drive its switches. The microcontroller generates the input pulse for the driver circuit by taking the input signals from the load. From the output of driver, the pulses are given to gate of the MOSFET switches. The hardware connections are made as per the circuits developed and is shown in Figure 20. The input voltages of +24 V and +36 V are given using RPS. The output of MCT2E generates the pulse with different pulse widths to trigger the input and output switches of the two input two outputs DC-DC converter which is shown in Figure 21.The corresponding closed loop output voltages V_{01} and V_{02} are shown in Figure 22. The transient and steady state errors are eliminated. The output voltages obtained across V_{01} and V_{02} are 83.2V and 39.5V respectively. Even with the change in the load current, output voltage is maintained constant.

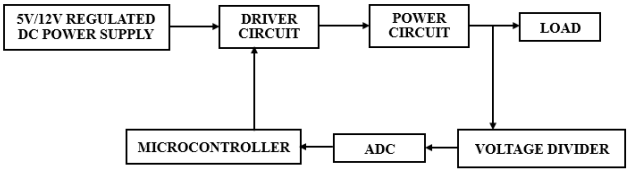

Figure 19. Hardware block diagram for closed loop system.

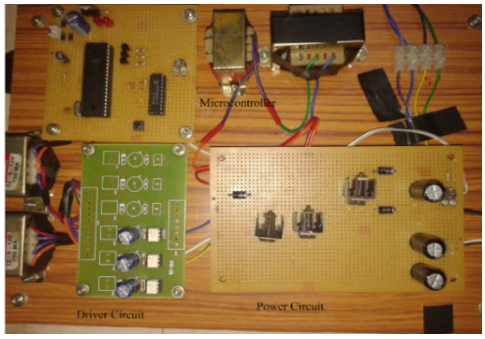

Figure 20. Hardware assembly.

Table 6. Hardware components with specifications

Components	Specifications
MOSFET	IRF840
Inductor	28mH
Capacitor	1000μF, 2200 μF
Driver IC	MCT2E
Regulator IC	IC 7805
ADC	ADC0804
Microcontroller	AT89S51
Diode	IN4007
Transistor	BC547

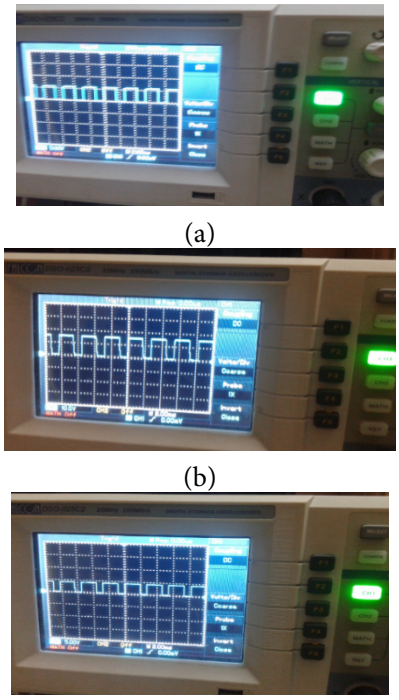

(a) (b) (c)

Figure 21. Gate drive pulse for switches (a) S_1, (b) S_2 and (c) S_3.

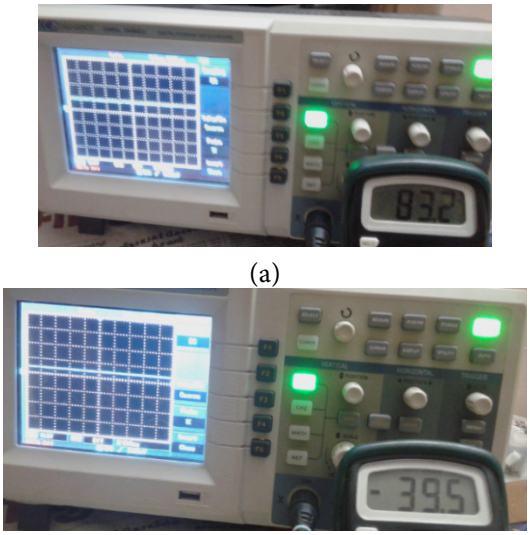

(a) (b)

Figure 22. Output voltage waveforms (a) (V_{01}) and (b) (V_{02}).

7. Conclusion

Asymmetric CHB-MLI fed from MIMO DC-DC boost converter using PV panel as one of its source has been proposed in this project work. The various analytical equations governing the PV cell are modelled and simulated. MPPT algorithm for PV model is developed to improve the efficiency of the system. Using two input two outputs DC-DC boost converter two different energy sources have been combined by which two different output voltages are produced. Its different modes of operation, steady state and dynamic characteristics have been studied. Compensators for the converter system using small signal modelling is designed and closed loop operation for MIMO converter has been performed. Thus the stability is achieved and the steady state error is removed. This converter system is fed to asymmetric CHB-MLI. Its THD value is observed to analyze about the performance of the system. To verify the simulation results, hardware implementation is done for two input two outputs DC-DC boost converter under closed loop condition.

8. References

1. Modeling and Circuit-Based Simulation of Photovoltaic arrays.http://ieeexplore.ieee.org/document/5347680/. Date Accessed: 27/09/2009.
2. Hamrouni N, Chérif A. Modeling and Control of a Single-Phase Grid Connected Photovoltaic System.Revue des Energies Renouvelables.2007 Sep;10(3):335-44.
3. Kuo YC, Liang TJ, Chen JF. Novel Maximum-Power-Point-Tracking Controller for Photovoltaic Energy Conversion System.IEEE Transactions on Industry Applications.2001 Jun;48(3):594–601.
4. Optimized Maximum Power Point Tracker for Fast-Changing Environmental Conditions.http://ieeexplore.ieee.org/document/4677275/. Date Accessed: 30/06/2008.
5. Tao H, Kotsopulous A, Duarte JL, Hendrix MAM. Family of multiport bidirectional DC-DC converters. IEE Proceedings - Electric Power Applications. 2006 May;153(3):451–58. https://doi.org/10.1049/ip-epa:20050362
6. Mahalakshmi R, Sindhu Thampatty K C. Implementation of Grid Connected PV array using Quadratic DC-DC Converter and Single Phase Multi Level Inverter. Indian Journal of Science and Technology.2015 Dec;8(35):1–7. https://doi.org/10.17485/ijst/2015/v8i35/80548
7. Bhuvaneshwari V, Harikumar ME, ShakilAhmed A, Vinoth R, Singh AB. Multicarrier Sinusoidal PWM Technique Based Analysis of Asymmetrical and Symmetrical 3Φ Cascaded MLI.International Journal of Advanced Research in Computer and Communication Engineering.2014 Nov;3(2):5755-61.
8. Seyezhai R, Mathur BL. Hybrid Multilevel Inverter using ISPWM Technique for Fuel Cell Applications.International Journal of Computer Applications.2010 Nov;9(1):41–47 . https://doi.org/10.5120/1347-1817
9. Kyocera. https://en.wikipedia.org/wiki/Kyocera. Date Accessed: 09/09/2016.
10. Sridhar N, Kanagaraj R. Modeling and Simulation of Controller for Single Phase and Three Phase PWM Rectifiers. Indian Journal of Science and Technology.2015 Nov;8(32):1–8. https://doi.org/10.17485/ijst/2015/v8i32/87869
11. Krishna S, Reddy M, Kalyani M, Elangovan D. U. A Small Signal Analysis of DC-DC Boost Converter. Indian Journal of Science and Technology.2015 Jan;8(S2):1–6. https://doi.org/10.17485/ijst/2015/v8iS2/57787
12. Ahmadi R, Ferdowsi M. Double-Input Converters Based on H-Bridge Cells: Derivation, Small-Signal Modeling, and Power Sharing Analysis.IEEE transactions on Circuits and Systems—I: regular papers.2012 Apr;59(4):875–88 . https://doi.org/10.1109/TCSI.2011.2169910
13. Chaudhari H N, Patel D. Comparison of Asymmetrical Cascaded Multilevel Inverter Control Techniques. International Journal of Innovations in Engineering and Technology.2013 Jun;2(3):31–36.
14. Seyezhai R. A Comparative Study of Asymmetric and Symmetric Cascaded Multilevel Inverter employing variable Frequency Carrier based PWM.International Journal of Emerging Technology and Advanced Engineering.2012 Mar;2(3):230–7.
15. Rauschenbach H S. Solar cell array design handbook. Van Nostrand Reinhold:Newyork.1980. https://doi.org/10.1007/978-94-011-7915-7 PMid:9537054
16. Giuseppe C, Gardella S, Marchesoni M, Salutari R, Sciutto G. A New multilevel PWM method: A theoretical analysis. IEEE Trans on power Electronics.1992 Jul;(3):497–505.
17. Liu YC, Chen YM. A systematic approach to synthesizing Multi-Input DC-DC converters. IEEE Transactions on Power Electronics.2009 Jan;24(1):116–27. https://doi.org/10.1109/TPEL.2008.2009170
18. Behjati H, Davoudi A. A Multiple-Input Multiple-Output DC–DC Converter.IEEE Transactions on industry applications.2013 May-Jun;49(3):1464–79. https://doi.org/10.1109/TIA.2013.2253440